Thermal Science and Engineering (2022) Volume 5 Issue 1
doi:10.24294/tse.v5i1.1526

ORIGINAL RESEARCH ARTICLE

Numerical simulation of the heat storage performance of aluminum/paraffin composite phase change materials

Baoming Chen*, Yanyong Zhang, Jiayang Liu

School of Thermal Engineering, Shandong Jianzhou University, Jinan 250101, Shandong province, China. E-mail: chenbm@sdjzu.edu.cn

ABSTRACT

Phase change energy storage materials are widely used in the fields of battery thermal management and solar power generation due to their characteristics of storing and releasing energy periodically. However, their further applications are limited by their low thermal conductivity. The addition of high thermal conductivity foams provides an effective method to address this shortcoming. A three-periodic minimal surface (TPMS) was used to generate an aluminum foam skeleton, and the variation of phase change heat storage of the aluminum/paraffin composite phase change material was numerically simulated based on the pore scale. The results showed that the addition of aluminum skeleton enhanced the heat storage and shortened the melting time, and the melting time of the composite phase change material was shortened by 68%, 75% and 80% when compared with pure paraffin wax at the porosity of 0.90, 0.85 and 0.80, respectively, and the temperature field was more uniform during the heat storage process, The thermal non-equilibrium effect between the aluminum skeleton and the paraffin wax is verified, and the lower the porosity of the aluminum/paraffin composite phase change material, the more obvious this effect is.

Keywords: Triple-periodic Minimal Surface; Aluminum Skeleton; Solid-liquid Phase Transition

ARTICLE INFO

Received: 9 February 2022
Accepted: 18 March 2022
Available online: 25 March 2022

1. Introduction

The increasing global energy demand, including the limited supply of fossil fuels and their harmful effects on the environment, has prompted the need for more sustainable, environmentally friendly, renewable energy sources, but both new energy sources, such as solar, wind energy, and waste heat from traditional industries, are cyclic and intermittent in nature. Therefore, energy storage technology has become a key technology to ensure efficient and stable operation of new energy and industrial waste heat recovery systems[1]. However, the low thermal conductivity of phase change materials (PCM) used in latent heat storage (LHS) systems severely impairs the rate of thermal energy storage and release. In order to improve the thermal performance of LHS systems, numerous performance enhancement studies have been conducted. The results of these studies provide valuable references for the performance improvement and optimization of LHS systems. Tauseef-ur-Rehman *et al.*[2] reviewed the enhanced heat transfer of phase change materials by highly thermally conductive porous materials, Drissi *et al.*[3] summarized the enhancement techniques to improve the thermal conductivity of paraffin waxes for low temperature phase change materials, Tao and He[4] reviewed the development and performance enhancement methods of PCMs in LHS systems. To overcome

the limitation of low thermal conductivity of PCMs, there are several main methods to enhance the thermal performance of phase change materials, including insertion of fins[5,6], addition of suspension agents[7,8], foam materials[9]. Among these technologies, foam materials are more effective in improving thermal conductivity due to their large surface area, high porosity, high thermal conductivity, high strength, and light weight. Numerous numerical simulations have been conducted on the solid-liquid phase change heat transfer process of foams from the pore scale and representative elementary volume (REV) perspective. In terms of REV scale, Krishnan *et al.*[10] proposed a two-temperature model considering the local thermal non-equilibrium effect between the metal matrix and PCM, and discussed the effects of Rayleigh number, Stefan number and interstitial Nusselt number on the melting performance of PCM. Tao *et al.*[11] conducted a numerical study of the LHS properties of copper foam/paraffin using a dual-temperature model. The effects of porosity and pore density on the melting rate, heat storage and heat storage density of the phase change material were investigated. Zhu *et al.*[12] applied the nonequilibrium equation to study the melting process of paraffin in aluminum foam. The heat loss, average liquid flow rate and latent heat storage efficiency were analytically discussed. The results showed that the thermal response of the composite could be improved by using aluminum foam with high PPI value or changing the shape of the cold wall.

In terms of the pore scale, the pore scale not only takes into account the complex geometry and pore-scale heat flow inside the skeleton and phase change material. Moreover, it is not necessary to find out the heat transfer coefficient between the metal skeleton and the phase change material, which is helpful to reduce the model prediction error caused by the uncertainty of heat transfer coefficient. In addition, the pore-scale method does not need to assume the thermal non-equilibrium between the skeleton and the phase change material. Therefore, compared with the REV-scale approach, the pore-scale approach is more reasonable for studying the melting process of composite phase change materials. Wang *et al.*[13] used a numerical method to construct a WP model consisting of six tetrahedra and two irregular dodecahedra based on the pore scale to simulate the melting heat transfer process of an open-cell foam metal at constant temperature. The results show that the porosity, thermal conductivity of the foam metal and the thermal conductivity of the phase change material have significant effects on the effective thermal conductivity of the composite phase change material, but the pore size has little effect on it. Abishek *et al.*[14] found that high porosity foam-metal composites are beneficial for improving and controlling the melting rate of phase change materials for thermal energy storage and process temperature control by investigating the effect of micromorphology on metal-foam-paraffin composites. Hu and Gong[15] used numerical methods to calculate the temperature change and melting process of composite phase change materials based on the pore scale, and investigated the effects of geometric parameters such as porosity and pore density of foam metals on the thermal properties of the composites. Sundarram and Li[16] developed a three-dimensional finite element model considering both metal and phase change material regions. The pore size and porosity effects of the PCM thermal management system as well as the system variables, such as heat production and heat dissipation of the system were investigated, and the results showed that both porosity and pore size have a significant effect on the heat storage of the phase change material. In this paper, based on the pore scale, the triply periodic minimal surface (TPMS) method was used to generate aluminum foam skeletons to investigate the effect of aluminum skeleton addition on the heat transfer of paraffin melting.

2. Physical model and mathematical model

2.1 Establishment of the three-dimensional physical model

In order to describe the structure of foam materials, many scholars have made a lot of simplifications of foam materials. Xu *et al.*[17] assumed the foam metal as a regular square structure in order to

simulate the influence of foam materials on the phase change process, and the model reflects the advantages of foam metal such as high porosity and large specific surface area, and because the model is more regular, the mesh division is simpler and the calculation is less. However, the description of the internal structure of the real foam material is not detailed enough. To describe the internal structure of the foam material more closely, Sundarram and Li[16] and Annapragada *et al.*[18] used the face-centered and body-centered methods to describe the foam material, but due to its irregular structure, the meshing is more difficult, the computational effort is larger, and the convergence is more difficult. The foam material used in this study is generated by the triply periodic minimal surface (TPMS)[19] method, which has been widely used in many fields due to its advantages of controllable porosity, pore size, pore shape, pore connectivity[20-23].

2.2 Introduction of triply periodic minimal surface (TPMS)

Minimal surfaces are described mathematically mainly in terms of area and curvature. The area is described as the smallest area that the model has under all constraints, and the curvature is described as a surface with zero mean curvature of the model, which is the average of the maximum and minimum curvature at any point in space, i.e., if the mean curvature at any point on the surface in space is zero, the surface is called a minimal surface. A triply periodic surface is one that exhibits periodic variation in all three directions in space: *X*, *Y*, and *Z*. Therefore, a triply periodic minimal surface is a surface that exhibits periodic variation in the *X*, *Y*, and *Z* directions in space and has zero mean curvature. The main methods to build TPMS are such as parametric method, boundary implicit method and surface method. TPMS has an exact parametric form, called Weierstrass formula, which is defined by equation (1):

$$x = R\int_{\omega_0}^{\omega} e^{i\theta}(1-\tau^2)S(\tau)d\tau$$

$$y = R\int_{\omega_0}^{\omega} e^{i\theta}(1+\tau^2)S(\tau)d\tau$$

$$z = R\int_{\omega_0}^{\omega} e^{i\theta}2\tau S(\tau)d\tau \tag{1}$$

Where: R is the real part of the imaginary number; ω is the complex variable; $S(\tau)$ is the function that varies with different surfaces.

Compared with the parametric TPMS form, implicit periodic surfaces have more advantages than the parametric TPMS form and can usually be defined as

$$\phi(r) = \sum_{k=1}^{k} A_k \cos\left[2\pi\left(h_k \cdot r\right)/\lambda_k + p_k\right] = C \tag{2}$$

Where: A_k is the amplitude factor, λ_k is the periodic wavelength, h_k is the kth lattice shed vector in space, r is the position vector in Euclidean space, p_k is the phase, C is the constant.

There are three common TPMS models, as shown in **Table 1**.

Table 1. TPMS model

TPMS	Mathematical expression
P	$cos(\omega_x x) + cos(\omega_y y) + cos(\omega_z z) = C$
D	$cos(\omega_x x)\,cos(\omega_y y)\,cos(\omega_z z) + sin(\omega_x x)\,sin(\omega_y y)\,sin(\omega_z z) = C$
G	$sin(\omega_x x)\,cos(\omega_y y) + sin(\omega_z z)\,cos(\omega_x x) + sin(\omega_y y)\,cos(\omega_z z) = C$

For a given TPMS surface, the corresponding TPMS entity is defined as $\{\varphi(x, y, z) \le 0, 0 \le x \le 1, 0 \le y \le 1, 0 \le z \le 1$, and the porosity of the TPMS entity is expressed as

$$\varepsilon = \left(1 - V_s / V\right) \times 100\% \tag{3}$$

Where: V_s is the volume of porous skeleton surrounded by TPMS entities, V is the total volume (pore volume and porous skeleton volume).

The pore size and porosity can be precisely controlled by adjusting the parameters ω and C in the TPMS expression. Specific operation steps:

(1) Determine the appropriate parameters ω and C according to the specific porosity;

(2) Write the code in Mathematical ware based on the determined mathematical expres-

sions and generate the model, which is exported to STL file;

(3) The exported STL file is imported into the finite element software COMSOL for calculation.

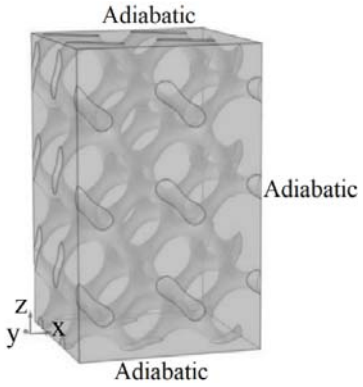

Figure 1. Physical model.

The physical model is shown in **Figure 1**, the size of the square cavity is L × W × H = 2.5 cm × 2.5 cm × 5.0 cm, the cavity is filled with TPMS generated aluminum skeleton, the left wall surface of the square cavity is the high temperature wall surface, the temperature t_h = 50 °C, the other walls are adiabatic, the initial temperature t_0 = 20 °C. The initial melting temperature is 71 °C and the temperature at the end of melting is 72 °C.

2.3 Mathematical modeling

The composite phase change material is very complex in the heat transfer process, including convective heat transfer between metal foam and liquid paraffin, heat transfer between metal foam and solid paraffin, natural convection of liquid paraffin, etc.

Table 2. Physical parameters

Material	Densityρ/(kg·m^{-3})	Specific constant pressure heat capacityc_ρ/(J·kg^{-1}·K^{-1})	Thermal conductivity k/(W·m^{-1}·K^{-1})	Latent heat L/(kJ·kg^{-1})	T_1/K	T_2/K
Aluminum skeleton	2,700	900	238.00	–	–	–
Paraffin liquid	860	2,177	0.26			
Paraffin wax solid	900	1,500	0.26	200	298	308

Several assumptions are made to simplify the calculations: (1) liquid paraffin is assumed to be an incompressible fluid and its flow is laminar in the closed space; (2) natural convection due to buoyancy is simulated using the Boussinesq assumption; (3) thermal radiation within the composite phase change material is neglected; (4) the density of aluminum foam is constant, and the physical properties are considered homogeneous and isotropic except for the density of paraffin; (5) the two phases interface is a coupled boundary condition (i.e., at thermal equilibrium), and the heat flow through the interface is driven by the temperature gradient between the two phases. Then the two-phase boundary satisfies:

$$T_f = T_s, k_f \frac{\partial T_f}{\partial n} = k_s \frac{\partial T_s}{\partial n} \tag{4}$$

Based on the assumptions, pore-scale numerical simulations are performed.

Control equations:

$$\frac{\partial \rho}{\partial t} + \nabla \cdot (\rho u) = 0 \tag{5}$$

Momentum equation.

$$\rho \frac{\partial u}{\partial t} + \rho (u \cdot \nabla) u = \nabla \cdot [-p\boldsymbol{I} + \mu(\nabla u + (\nabla u)^T) - \frac{2}{3}\mu(\nabla u)\boldsymbol{I}] + F \tag{6}$$

In Equations (4)–(6): p and T are the pressure and temperature of the phase change material, respectively, I is the vector of X, Y and Z coordinate directions and gravity is considered in the simulation, and F is the force source term, which consists of the drag force F_v generated in the paste zone and the thermal buoyancy force F_G generated by gravity, expressed as

$$F = F_v + F_G \tag{7}$$

$$F_{\mathrm{v}} = -\frac{(1-\theta)^2}{\theta^3+\lambda} A_{\mathrm{mush}} \cdot u \tag{8}$$

$$F_{\mathrm{G}} = \rho\beta g\left(T - T_{\mathrm{m}}\right) \tag{9}$$

In Equations (7)–(9): θ is the liquid phase fraction of the phase change material; A_{mush} and λ are the paste region constants, λ are generally taken as small values, mainly to prevent the denominator of Eq. The smaller the value, the higher the accuracy of the volume force, $\lambda = 10^{-3}$; A_{mush} are generally taken as larger values, $A_{\mathrm{mush}} = 6 \times 10^4$, these two paste zone constants are used to limit the development of the paste zone velocity; g is the acceleration of gravity; T_{m} is the temperature at which the phase transition occurs.

Energy equation:

$$\rho_{\mathrm{foam}}\, c_{p_{\mathrm{foam}}} \frac{\partial T}{\partial t} + \rho c_p \frac{\partial T}{\partial t} + \rho c_p u \cdot \nabla T = \nabla \cdot \left(k_{\mathrm{foam}} \nabla T + k \nabla T\right) \tag{10}$$

Where: ρ_{foam}, $c_{p_{\mathrm{foam}}}$, k_{foam} are the density, specific constant pressure heat capacity and thermal conductivity of the metal bubble, k, ρ and c_p are the equivalent thermal conductivity and equivalent specific constant pressure heat capacity of the phase change material paraffin, respectively, defined as

$$k = \theta \cdot k_{\mathrm{phasel}} + (1-\theta) \cdot k_{\mathrm{phase\ 2}} \tag{11}$$

$$\rho = \theta \cdot \rho_{\mathrm{phase\ 1}} + (1-\theta)\rho_{\mathrm{phase\ 2}} \tag{12}$$

$$c_p = \frac{1}{\rho}\left(\theta \cdot \rho_{\mathrm{phase\ 1}} c_{p_{\mathrm{phasel}}} + (1-\theta)\rho_{\mathrm{phase\ 2}} c_{p_{\mathrm{phase\ 2}}}\right) + L\frac{\partial \alpha_{\mathrm{m}}}{\partial T} \tag{13}$$

$$\alpha_{\mathrm{m}} = \frac{1}{2}\frac{(1-\theta)\rho_{\mathrm{phase\ 2}} - \theta\rho_{\mathrm{phase\ 1}}}{\theta\rho_{\mathrm{phasel}} + (1-\theta)\rho_{\mathrm{phase2}}} \tag{14}$$

Where: k_{phase1} is the thermal conductivity of solid paraffin, k_{phase2} is the thermal conductivity of liquid paraffin; ρ_{phase1} is the density of solid paraffin, ρ_{phase1} is the density; $C_{\rho_{phase1}}$ is the specific heat capacity of solid paraffin, $C_{\rho_{phase}}$ is the specific constant pressure heat capacity of liquid paraffin; L is the latent heat of phase change.

3. Mesh-independent validation

The COMSOL Multiphysics 5.4 software was used to generate unstructured meshes in the computational domain. The physical field controls the grid, the grid size is set to fine, normal, and coarse in turn, and the grid number is 2,394,441, 1,124,215, and 513,084 for grid independence analysis, as shown in **Figure 2**. When the porosity of the composite phase change material is 0.90, numerical simulation is carried out. Through the comparison of the calculation results under three different grid conditions, it was found that the difference in the time taken to melt completely between 1,124,215 and 2,394,441 grids was less than 5%. Taking into account the accuracy and time of numerical calculation, the number of grids is 1,124,215, and the result is not affected by the grid size.

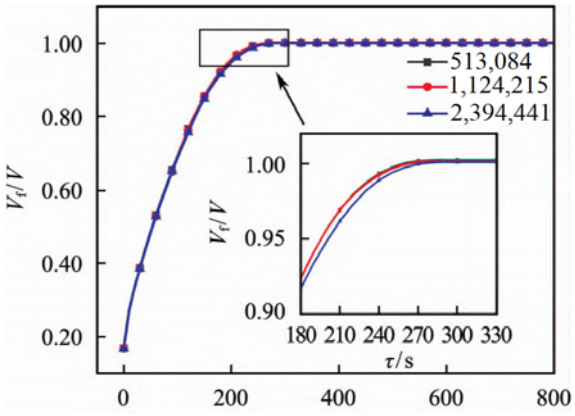

Figure 2. Mesh independence analysis.

4. Results and discussion

4.1 Effect of the presence of skeleton on the phase change heat storage process

Figure 3 shows the variation of phase field with time for the phase change of paraffin wax with/without skeleton. Red color in **Figure 3** indicates the melted liquid paraffin wax, blue color indicates the un-melted solid paraffin wax, and between red and blue color is the molten paraffin wax (paste region). **Figure 3(a)** shows the distribution of phase field with time for no skeleton, and **Figure 3(b)** shows the distribution of phase field with time for filled skeleton. For the pure paraffin phase transition, it can be seen from **Figure 3** that in the early

stage of melting, the solid-liquid interface is almost parallel to the left side of the hot wall, and the heat transfer is mainly in the form of heat conduction, with the paste area perpendicular to the upper and lower walls.

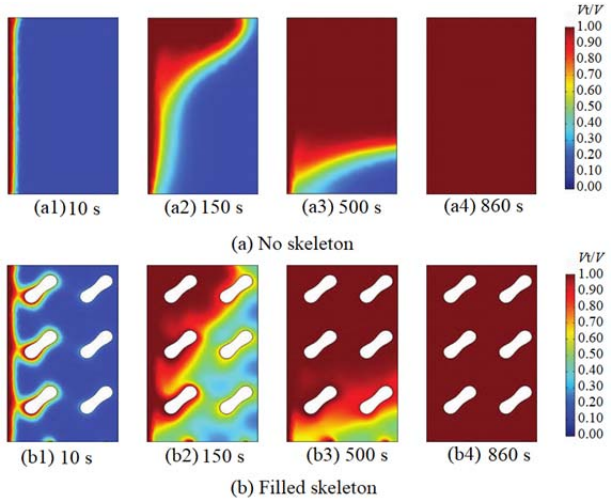

Figure 3. Phase field with or without framework changes with time.

With the phase change, the volume expansion caused by the difference in density between the solid-liquid phase of paraffin wax, the liquid paraffin wax gradually increases in volume and starts to flow upward under the action of the thermal buoyancy force, the natural convective heat transfer becomes more obvious and the paste zone becomes inclined. For the phase change material filled with aluminum skeleton, the addition of the aluminum foam skeleton increased the effective thermal conductivity of the composite phase change material substantially, but its skeleton structure also inhibited the flow of liquid paraffin in it to a certain extent, which prevented the movement of liquid high temperature paraffin to the top of the solid paraffin, and the addition of high thermal conductivity skeleton obviously accelerated the phase change process and shortened the phase change melting The addition of a high thermal conductivity skeleton significantly accelerated the phase change process and shortened the phase melting time. Comparing the phase field diagrams with and without the skeleton at the same time, it can be seen that the addition of the skeleton thickened the paste zone of the paraffin, mainly because the addition of the high thermal conductivity skeleton made the heat transfer from the left side of the high temperature wall more rapid, which accelerated the melting of the overall paraffin in the square cavity, and the same phenomenon was observed in the experiments conducted by Chen *et al.*[24] with an infrared camera.

Figure 4 shows that the effect of the skeleton on the heat storage of paraffin melting is different when the porosity of the composite phase change material varies. The melting time of pure paraffin wax is 860 s, and the complete melting time of aluminum/paraffin wax composite phase change material with porosity of 0.90, 0.85, 0.80 is 270, 210, 170 s, respectively, compared with pure paraffin wax. The melting times of the composite phase change materials were reduced by 68%, 75% and 80%, respectively, compared to pure paraffin. The addition of aluminum bones to the framework increased the effective thermal conductivity of the composite phase change material due to its much higher thermal conductivity than paraffin wax, which in turn enhanced the thermal storage of paraffin wax phase change material. The lower the porosity of the composite phase change material, the higher the proportion of its skeleton part, the higher the effective thermal conductivity, and therefore the faster the melting rate.

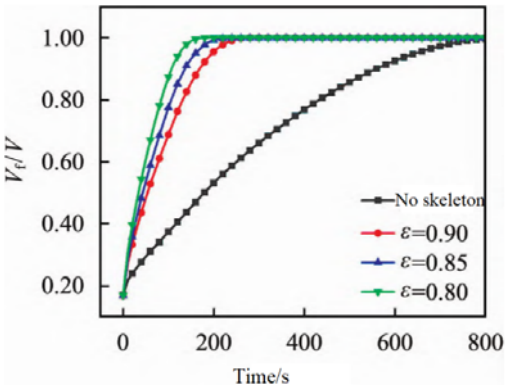

Figure 4. Change of liquid phase ratio with time.

4.2 Thermal non-equilibrium effect between the foam and the phase change material

To investigate the thermal non-equilibrium phenomenon inside the composite PCM, **Figure 5** shows the difference between the average temperature of the skeleton and the average temperature of the phase change material at x = 1 cm as a function of time. The results indicate that there is a thermal nonequilibrium effect in the melting process of the

composite phase change material.

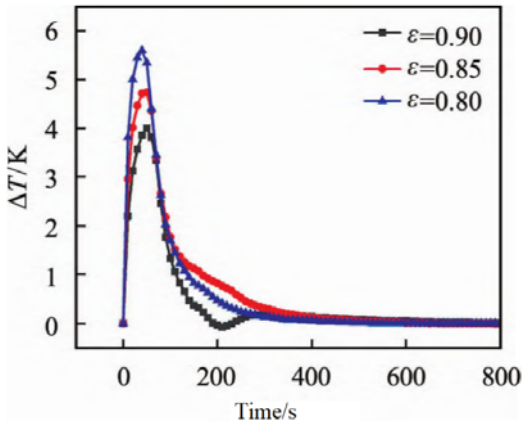

Figure 5. Temperature difference change with time.

At the beginning of the melting process, the temperature difference increases rapidly, mainly because the heat transfer through the highly thermally conductive aluminum skeleton is faster, and the aluminum skeleton heats up quickly, while the heat transfer through the solid paraffin wax is slower due to its lower thermal conductivity. As the melting proceeds, the temperature difference starts to decrease, mainly due to the transfer of heat from the aluminum skeleton to the surrounding paraffin and the natural convective heat transfer from the liquid paraffin. The difference between the average temperature of the skeleton and the average temperature of the phase change material finally decreases to 0 K due to the enhanced natural convection of paraffin in the liquid state. As the porosity of the composite PCM decreases, the local thermal non-equilibrium effect becomes more obvious, mainly because the smaller the porosity is, the larger the heat transfer surface area of the aluminum skeleton will be, resulting in a more rapid heat transfer through the aluminum skeleton.

4.3 Effect of aluminum skeleton addition on the temperature field of composite phase change material

Figure 6(a) shows the temperature distribution of the pure phase change material, paraffin wax, with time. The temperature shows an obvious gradient distribution, due to the low thermal conductivity of pure paraffin wax, poor heat conduction ability, and the influence of natural convection heat buoyancy force, the temperature at the top left is higher than that at the bottom right, resulting in the accumulation of temperature at the top. The melting process of the composite phase change material is shown in **Figure 6(b)**, and the temperature does not accumulate in the upper left corner obviously.

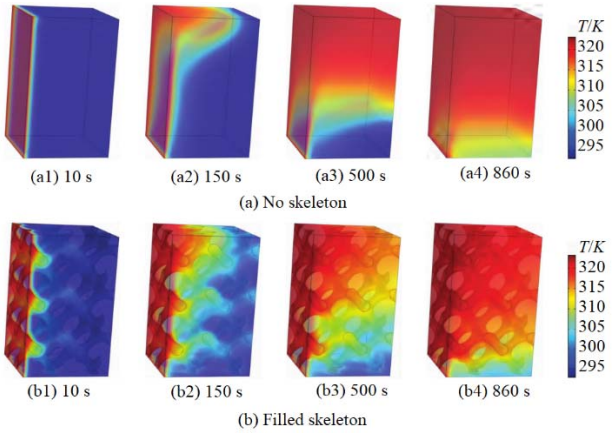

Figure 6. Phase field with or without framework changes with time.

This phenomenon is due to the high thermal conductivity of aluminum foam, which facilitates rapid heat transfer and thus homogenizes the temperature throughout the composite. Compared with pure paraffin, the temperature distribution in the composite PCM is more uniform and the melting time is shorter. The heat storage property of the phase change material can be fully utilized for heat storage.

In order to investigate the uniformity of the internal temperature field of the composite phase change material, the temperatures of three points in the vertical direction were extracted under the condition of 0.85 porosity of the composite phase change material, and the coordinate points were T_1 (1.00, 1.75, 0.80), T_2 (1.00, 1.75, 2.00), and T_3 (1.00, 1.75, 3.20). **Figure 7** shows the temperature variation of the skeleton-free characteristic points with time, it can be seen that the temperature difference between the three points is very large, it takes 80 s for T_1, 260 s for T_2 and 520 s for T_3 to reach the phase change temperature, the time taken to reach the phase change at T_3 is 6.50 times that of T_1, the time difference is 440 s, which is 2.00 times that of T_2, and the time difference is 250 s. The phase transition response times after adding the aluminum skeleton were 20, 40, 70 s, respectively, and the

phase transition response times T_3 were 3.50 and 1.75 times of T_1, T_2, with time differences of 50 and 30 s, respectively. It can be seen that the composite phase change material not only melts faster, but also has a more uniform temperature field distribution compared to pure paraffin.

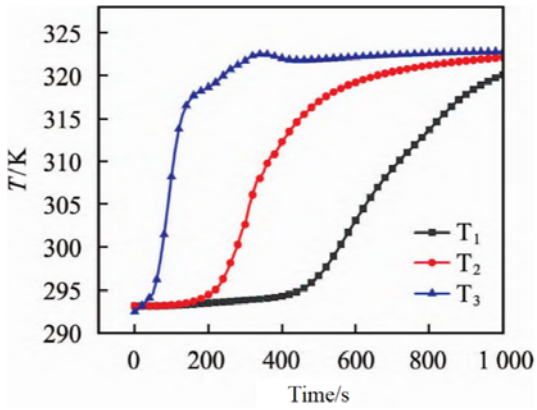

Figure 7. Temperature curve of characteristic points without skeleton.[26]

The temperature difference along the vertical direction in the phase change heat storage process between the composite and pure paraffin is mainly due to the fact that the paraffin wax near the heating wall melts first, accompanied by volume expansion, driven by the thermal buoyancy force and the density difference, the liquid high temperature paraffin wax moves upward to the top surface of the paraffin material, so that the temperature distribution in the height direction is more different. In contrast, in the aluminum foam/paraffin composite phase change material, the temperature difference along the height direction is significantly smaller than that of the single paraffin wax, which is caused by the difference in the heat transfer mode within the two materials. The presence of the aluminum foam skeleton in the composite makes the velocity field development of the liquid paraffin within the material limited and the natural convection weakened, while the high thermal conductivity of the foam skeleton makes the overall heat transfer mode of the composite phase change material conductive. In the phase change heat storage process of the two different phase change materials, liquid paraffin waxes both flow to the top surface, but due to the higher effective thermal conductivity of the composite phase change material, the heat can be transferred more quickly through the foam skeleton to the lower low temperature region of the material, resulting in a significantly reduced temperature difference in the height direction and a more uniform temperature distribution than that of the single paraffin wax. The heat transfer mode of the monolithic paraffin is mainly natural convection, the liquid paraffin is driven upward by the thermal buoyancy force, which causes the formation of heat accumulation in the upper part of the paraffin material with a larger temperature rise rate, while the lower part has a slower temperature rise rate due to the low thermal conductivity of the solid paraffin, therefore, the temperature of the monolithic paraffin in the height direction is lower than that of the composite phase change material.

4.4 Effective thermal conductivity of aluminum/paraffin composite phase change materials

Although the effective thermal conductivity does not reveal the phase change process, it helps to describe the macroscopic heat transfer phenomena. Although this structure in the paper is different from the real framework of foam metals, it can be properly used to analyze the heat transfer in media with high porosity.

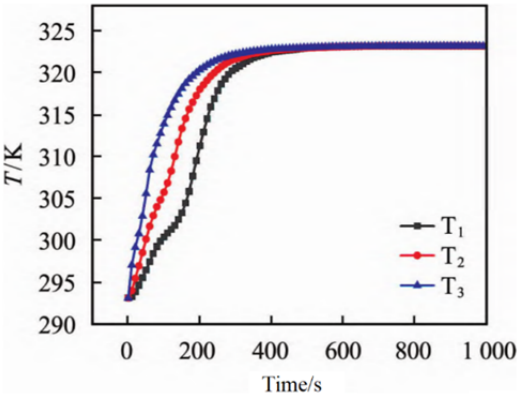

Figure 8. Temperature curve of characteristic points with skeleton.

The effective thermal conductivity of aluminum/paraffin composites is calculated by numerical simulations at steady state for different porosity conditions. The upper and lower walls of the square cavity are at constant temperatures of 320 and 310 K, respectively, both of which are greater than the temperature T_2 at complete melting, and the other walls are adiabatic, and to simplify the calculations,

the following assumptions are used: (1) the heat transfer is mainly one-dimensional heat conduction; (2) the heat flow in any section is equal along the heat transfer direction. The thermal conductivity λ can be solved according to the Fourier equation:

$$\Phi = -A\lambda_e \frac{\mathrm{d}T}{\mathrm{d}x} \tag{15}$$

The heat flow density and temperature gradient at the lower wall are calculated in COMSOL software, and the effective thermal conductivity of the aluminum/paraffin composite phase change material is calculated using equation (15), as shown in **Figure 9**. The thermal conductivity of paraffin is 0.26 W/(m·K). The effective thermal conductivity of the composite phase change material is 16.84, 12.26, 8.84 W/(m·K) for a porosity of 0.80, 0.85, 0.90, respectively, which are 64, 47, 34 times than that of pure paraffin wax. The results show that the composite phase change material can significantly improve the thermal conductivity, and the effective thermal conductivity decreases with the increase of porosity. The numerical simulation results in this paper compare well with the theoretical models established by Bhattacharya *et al.*[25] and Singh *et al.*[26], and the predicted results are in good agreement.

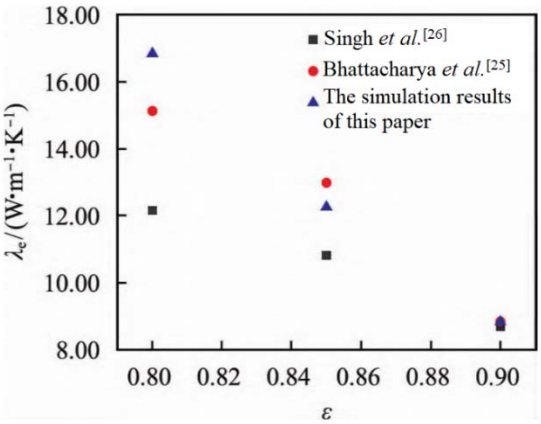

Figure 9. Comparison of simulated effective thermal conductivities and literature results.

5. Conclusion

(1) The TPMS method is used to generate the aluminum foam skeleton model, which is easy to use for enhanced thermal storage simulations and experiments due to its advantages of controllable porosity, pore size, pore shape, and pore connectivity, providing a more accurate and effective means for enhanced thermal storage.

(2) The presence of skeleton has a great influence on the phase change thermal storage process. The addition of high thermal conductivity aluminum skeleton material shortens the melting time, and with the decrease of porosity, the melting time is further shortened; the paraffin wax near the aluminum skeleton melts first and the paste area becomes thicker. The melting time of the composite phase change material was shortened by 68%, 75% and 80% compared to pure paraffin wax when the porosity of the composite phase change material was 0.90, 0.85 and 0.80, respectively.

(3) Thermal non-equilibrium phenomenon exists between aluminum foam and paraffin wax during melting process, with the increase of porosity and melting time, the temperature difference between paraffin wax and aluminum skeleton decreases and the thermal non-equilibrium effect decreases.

(4) The addition of high thermal conductivity aluminum skeleton not only accelerates the phase change of paraffin, but also promotes more uniform heat storage of the phase change material in the cavity, and the temperature uniformity of the composite phase change material is significantly stronger than that of the pure paraffin phase change material in the vertical direction.

Acknowledgement

This work was supported by the National Natural Science Foundation of China (51976111).

Conflict of interest

The authors declared that they have no conflict of interest.

References

1. Sharma RK, Ganesan P, Tyagi VV, *et al.* Developments in organic solid-liquid phase change materials and their applications in thermal energy storage. Energy Conversion and Management 2015; 95: 193–228.
2. Tauseef-ur-Rehman, Ali HM, Janjua MM, *et al.* A critical review on heat transfer augmentation of phase change materials embedded with porous ma-

terials/foams. International Journal of Heat and Mass Transfer 2019; 135: 649–673.
3. Drissi S, Ling TC, Mo KH. Thermal efficiency and durability performances of paraffinic phase change materials with enhanced thermal conductivity—A review. Thermochimica Acta 2019; 673: 198–210.
4. Tao Y, He Y. A review of phase change material and performance enhancement method for latent heat storage system. Renewable and Sustainable Energy Reviews 2018; 93: 245–259.
5. Shojaeefard MH, Molaeimanesh GR, Ranjbaran YS. Improving the performance of a passive battery thermal management system based on PCM using lateral fins. Heat and Mass Transfer 2019; 55(6): 1753–1767.
6. Arshad A, Ali HM, Khushnood S, *et al.* Experimental investigation of PCM based round pin-fin heat sinks for thermal management of electronics: Effect of pin-fin diameter. International Journal of Heat and Mass Transfer 2018; 117: 861–872.
7. Akhmetov B, Navarro ME, Seitov A, *et al.* Numerical study of integrated latent heat thermal energy storage devices using nanoparticle enhanced phase change materials. Solar Energy 2019; 194: 724–741.
8. Kean TH, Sidik NAC, Asako Y, *et al.* Numerical study on heat transfer performance enhancement of phase change material by nanoparticles: A review. Journal of Advanced Research in Fluid Mechanics Thermal Sciences 2018; 45(1): 55–63.
9. Alshaer WG, Nada SA, Rady MA, *et al.* Thermal management of electronic devices using carbon foam and PCM/nano-composite. International Journal of Thermal Sciences 2015; 89: 79–86.
10. Krishnan S, Murthy JY, Garimella SV. A two-temperature model for solid-liquid phase change in metal foams. Journal of Heat Transfer 2005; 127(9): 995–1004.
11. Tao Y, You Y, He Y. Lattice Boltzmann simulation on phase change heat transfer in metal foams/paraffin composite phase change material. Applied Thermal Engineering 2016; 93: 476–485.
12. Zhu F, Zhang C, Gong X. Numerical analysis and comparison of the thermal performance enhancement methods for metal foam/phase change material composite. Applied Thermal Engineering 2016; 109: 373–383.
13. Wang G, Wei G, Xu C, *et al.* Numerical simulation of effective thermal conductivity and pore-scale melting process of PCMs in foam metals. Applied Thermal Engineering 2019; 147: 464–472.
14. Abishek S, King AJC, Nadim N, *et al.* Effect of microstructure on melting in metal-foam/paraffin composite phase change materials. International Journal of Heat and Mass Transfer 2018; 127: 135–144.
15. Hu X, Gong X. Pore-scale numerical simulation of the thermal performance for phase change material embedded in metal foam with cubic periodic cell structure. Applied Thermal Engineering 2019; 151: 231–239.
16. Sundarram SS, Li W. The effect of pore size and porosity on thermal management performance of phase change material infiltrated microcellular metal foams. Applied Thermal Engineering 2014; 64(1-2): 147–154.
17. Xu W, Yuan X, Li Z. Study on effective thermal conductivity of metal foam matrix composite phase change materials. Journal of Functional Materials 2009; 8(10): 1329–1337.
18. Annapragada SR, Murthy JY, Garimella SV. Permeability and thermal transport in compressed open-celled foams. Numerical Heat Transfer Part B: Fundamentals 2008; 54(1): 1–22.
19. Giannitelli SM, Accoto D, Trombetta M, *et al.* Current trends in the design of scaffolds for computer-aided tissue engineering. Acta Biomater 2014; 10(2): 580–594.
20. Yoo DJ. Porous scaffold design using the distance field and triply periodic minimal surface models. Biomaterials 2011; 32(31): 7741–7754.
21. Yoo D. Heterogeneous minimal surface porous scaffold design using the distance field and al basis functions. Medical Engineering &Physics 2012; 34(5): 625–639.
22. Kapfer SC, Hyde ST, Mecke K, *et al.* Minimal surface scaffold designs for tissue engineering. Biomaterials 2011; 32(29): 6875–6882.
23. Elomaa L, Teixeira S, Hakala R, *et al.* Preparation of poly (epsilon-caprolactone)-based tissue engineering scaffolds by stereolithography. Acta Biomater 2011; 7(11): 3850–3856.
24. Chen Z, Gao D, Shi J. Experimental and numerical study on melting of phase change materials in metal foams at pore scale. International Journal of Heat and Mass Transfer 2014; 72: 646–655.
25. Bhattacharya A, Calmidi VV, Mahajan RL. Thermophysical properties of high porosity metal foams. International Journal of Heat and Mass Transfer 2002; 45(5): 1017–1031.
26. Singh R, Kasana HS. Computational aspects of effective thermal conductivity of highly porous metal foams. Applied Thermal Engineering 2004; 24(13): 1841–1849.